

Thermodynamic Modeling and Analysis of a Novel Multi-Generation Energy System Based on Gas and Wind Turbine

R. Bagheri^{1,*}, M. Soltani², R. Jamalpour³

¹Department of Mechanical Engineering, Karaj Branch, Islamic Azad University, Karaj, Iran.

²Department of Energy Systems Engineering, South Tehran Branch, Islamic Azad University, Tehran, Iran.

³Department of Civil Engineering, Karaj Branch, Islamic Azad University, Karaj, Iran.

Received: 24 February 2023 - Accepted: 07 May 2023

Abstract

A novel hybrid multi-generation system consisting of the following parts is proposed and thermodynamically analyzed: one gas turbine, one wind turbine, a district hot water, and a heat pump system for district heating, and a proton exchange membrane (PEM) electrolyzer to produce hydrogen as energy storage. This modeling is based on both one steam Rankine cycle and one organic Rankine cycle. The analysis for both energy and exergy is conducted, in order to comprehend the system performance, where values of 80.19% and 52.63% for energy and exergy efficiencies are found, respectively. Also an environmental impact assessment is performed and the effect of some parameters (ambient temperature, air compressor pressure ratio and wind speed) on carbon dioxide emission is investigated. During our investigation, some fuel is examined for combustion and fuel changes are reported. Furthermore, a study on the influence of enhancing renewable energy and reducing conventional system portion on production of a specified amount of electricity in an integrated system is carried out.

Keywords: Gas Turbine, Multi-Generation System, Exergy Efficiency, Wind Turbine, CHP Systems.

1. Introduction

Conventional fossil energy sources were used to be considered inexhaustible sources of energy. Now we know that they are not renewable and also cause global warming through emissions of greenhouse gases, particularly carbon dioxide. Therefore, two main challenges are ahead of us. The first challenge is the optimization of consumption of the remaining limited fossil fuels. This is achievable through enhancing system efficiencies and reduction of thermal energy losses. This is possible if we utilize several integrated systems called multi-generation energy systems [1]. The second challenge could be achieved by gradual replacement of fossil fuels with renewable energy sources. Reza Soltani et al [2] modeled a multi-generation energy system having one input (biomass fuel) and five products (electricity, steam, hot water, district hot water and wood dryer). They carried out a thermodynamic analysis and investigated the effect of each sub-system on both energy and exergy efficiencies. Ahmadi et al [3], modeled an integrated energy system including a micro gas turbine, a dual pressure heat recovery steam generator, an absorption chiller, a domestic water heater and a proton exchange membrane electrolyzer; this model had an ejector refrigeration cycle. They analyzed the system thermodynamically, trying to optimize the system, following two goals; total cost rate of the system and the system exergy efficiency.

Ratlamwala et al [4] proposed a new multi-generation geothermal-based double flash power generation, quadruple the absorption effect and the electrolyzer system. They analyzed the effects of geothermal source pressure and temperature, the effect of geothermal source mass flow rate, and the effect of ambient temperature on both energy and exergy efficiencies. They showed that an increase in the temperature, pressure and mass flow rate of the geothermal source, results in an increase in both power generation and hydrogen production rate and also leads to a reduction of the cooling load. Environmental impact is a significant parameter in conventional systems. Ahmadi et al [5] assessed thermodynamically a novel multi-generation energy system consisting of a biomass combustor, an organic Rankine cycle (ORC), an absorption chiller and a proton exchange membrane electrolyzer and a domestic water heater for hot water production. They investigated the environmental impact of the multi-generation energy system and compared the carbon dioxide emissions of this system with power generation system. Mago et al [6] show a Combine cooling, heating, and power (CCHP) system which uses waste heat from on-site electricity generation for a large office building and analyze its primary energy consumption, operational costs, and carbon dioxide emissions. They also compare it with conventional energy systems under the same applications. Renewable energy sources are capable of satisfying our present and future needs for energy. However, there are problems in consumption of these renewable energy sources.

*Corresponding author

Email address: r.bagheri@kiaau.ac.ir

For instance, wind energy systems do not produce usable energy during a significant portion of the year. This is due to a main problem, which is the production of electricity is dependent on wind blow which doesn't occur all the time at a constant and desirable speed. In general, the accessibility of solar and wind energy do not match with the time and the distribution of demand.

The independent use of the systems result in considerable over-sizing of system reliability, which in turn makes the design costly. Ozlu and Dincer [7] studied a solar-wind hybrid multi-generation system and investigated the effect of several input conditions on the system performance. They showed that energy and exergy efficiencies are higher than equivalent single energy systems. The system has 43% maximum energy efficiency and 65% maximum exergy efficiency. Bicer and Dincer [8] proposed a new renewable energy based multi-generation system, which integrates a solar PV/T system and a geothermal energy system, in order to produce electricity and heat for purposes like heating, cooling, making water hot and drying air. They also assessed the performance of the system by energy and exergy analysis methods; for a selected common case, overall energy and exergy efficiencies of 11% and 28% were obtained, respectively.

Ozturk and Dincer [10] analyzed a renewable-based multi-generation energy production system which produces power, heating, cooling, hot water, hydrogen and oxygen. They showed the effects of varying operating conditions (e.g. Reference temperature, direct solar radiation and receiver temperature) on the exergy efficiencies of the sub-systems as well as the whole system.

They also found that the parabolic dish collectors have the highest exergy destruction rate among the constituent parts of the solar-based multi-generation system. This was due to high temperature difference between the working fluid and the collector receives. In this paper, we propose a novel multi-generation system, based on a conventional energy (gas turbine) and a renewable energy system (wind turbine) which produces three commodities: electricity, heating and hot water. The main purposes of utilization of this multi-generation system are to enhance efficiency, sustainability, and to also reduce environmental impact. We also analyzed the effect of wind energy portion enhancing and reduction of portion of conventional energy, in order to provide a specified amount of electricity. These steps are listed as follows:

- Modeling and simulation of the multi-generation system
- Performing a thermodynamic and environmental analysis of the system.

- Parametric assessment of the effects of varying selected design parameters on exergy and energy efficiencies.

2. System Description

The proposed multi-generation system is shown in Fig. (1). It satisfies the needs of district electricity, heating, hot water and hydrogen illustrates an integrated multi-generation system including an air compressor, a combustion chamber, a gas turbine, a high temperature boiler (HTB) which produces steam Rankine cycles vapor, the waste heat from the cycle is used for obtaining heating for heat pump system, low temperature boiler(LTB) produce heating as an evaporator for organic Rankine cycle and waste heat from this cycle is used for obtaining hot water to district users and Wind turbines also produce electricity when there is enough wind and when there is extra energy it run the electrolyzer to produce hydrogen to storage for peak hours of electricity consumption.

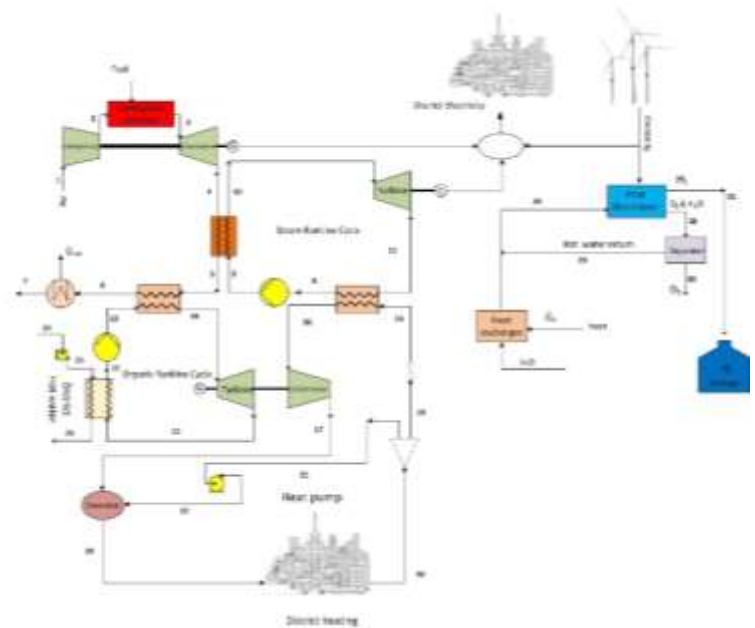


Fig. 1. Configuration of the multi-generation system.

Air enters the air compressor at ambient condition at point 1 and exits after compression (point 2). The hot air enters the combustion chamber into which fuel is injected, and hot combustion gases exit (point 3) and pass through a gas turbine, in order to produce power. The hot gas expands in the gas turbine to point 4. Hot flue of gases enters the high temperature boiler (HTB), in order to provide superheated steam for the steam Rankine cycle at point 10 and exit at a temperature of 579.3 °C (point 5). In low temperature boiler (LTB), the hot gases provides superheated fluid for ORC at point 14, and exit the heat exchanger at a temperature of 105.2 °C (point 6). In the last heat recovery, the

flue gas has provided heating for water electrolyzer and goes out at a temperature of 100 °C (point 7). The waste heat from the steam Rankine cycle condenser obtains hot water for the heat pump system and waste heat of ORC obtain district hot water at a temperature of 65 °C for district heating (point 26). We determine the enthalpy, energy and exergy of streams, using four main balances: mass, energy, entropy, and exergy. Energy and exergy balance equations are solved via ENGINEERING EQUATION SOLVER (EES) software. The thermodynamic modeling is based on some assumptions and input data.

Table. 1. The input parameters used to model the system.

Brayton Cycle	
Air mass flow rate	1.5(kg/s)
Fuel	Methane(CH_4)
Pressure ratio	12
Gas turbine inlet temperature	1173(°C)
Steam Rankine cycle	
Pump inlet temperature	70(°C)
Pump pressure	2000(kPa)
Pinch point temperature	10(°C)
ORC	
Pump inlet temperature	70(°C)
Pump pressure	2000(kPa)
Pinch point temperature	10(°C)
Working fluid	Cyclohexane
Heat pump system	
Evaporator output temperature	90(°C)
Compressor outlet pressure	270(kPa)
Working fluid	Water
Wind turbine	
Number of wind turbine	4
Diameter	34(m)[7]
Average wind speed	6.7(m/s)
Power coefficient	60%[7]
PEM electrolyzer	
λ_a	14[12]
λ_c	10[12]
T_{PEM}	80(°C)
L	100(μm)[12]

The assumptions for the system are as follows:

- All processes and components operate at steady state.
- Heat loss from the combustion chamber is considered to be 3% of the fuel lower heating value and all other components are adiabatic.
- Assuming that the combustion products can be modeled using the properties of pure air.
- The temperature at which district users use hot water is assumed to be the mean of the incoming and exiting temperatures (T_{avg}).
- Pinch point temperature of heat exchangers is 10 (°C).
- There are no pressure drop in the all processes.

- The ambient condition is $P_0 = 1.01$ bars and $T_0 = 298.15$ °K.
- The gas turbine operating with 88% efficiency at ISO condition. [14]
- The compressors and pumps operating with 85% efficiency at ISO condition. [14]
- The electrolyzer operates with 60% efficiency.
- Wind turbine operates with 90% efficiency. [11]
- Wind turbine operates with the average Manjil (Iran) wind Speed.
- The working fluid of organic Rankine cycle is Cyclohexane.

3. Thermodynamic Modeling and Analysis

The thermodynamic modeling of the proposed multi-generation system is described in this section, following a conventional control volume thermodynamic analysis approach, but pointing out important points specific to the present analysis. For this purpose, the system is divided into the following subsystems: (1) Brayton Cycle, (2) Steam Rankine Cycle, (3) Organic Rankine Cycle (ORC), (4) District Hot Water, (5) Heat Pump System, (6) Wind Turbine, (7) Proton Exchange Membrane (PEM) electrolyzer. Mass, energy and exergy rate balances are written for the system and its components in order to determine the energy input/output rate the exergy destruction rate, and the energy and exergy efficiencies. According to the conservation of mass principle, the mass entering the control volume is equal to the mass exiting the control volume. Accordingly general mass balance with assumption of steady state condition can be obtain as follows:

$$\sum \dot{m}_i = \sum \dot{m}_e \quad \text{Eq. (1)}$$

where \dot{m} is the mass flow rate, and the subscript i denotes inlet and e outlet.

Energy rate balances respectively can be written as follows:

$$\dot{E}_i = \dot{E}_e \quad \text{Eq. (2)}$$

The energy efficiency of the system and its components can be expressed as the ratio of the net energy output as products to the net input primary energy, as follows:

$$\eta = \frac{\dot{E}_e}{\dot{E}_i} \quad \text{Eq. (3)}$$

3.1. Brayton Cycle

3.1.1. Air Compressor (AC):

Air at ambient state enters the compressor. The compressor outlet air properties are dependent on the compressor is entropic efficiency and the compressor pressure ratio:

$$\dot{W}_{AC} = \dot{m}_a (h_2 - h_1) \quad \text{Eq. (4)}$$

Here, the subscript a refers to Air

3.1.2. Combustion Chamber (CC):

The flue gas properties are dependent on the air mass flow ratio and the fuel lower heating value (LHV)

$$\dot{m}_a h_2 + \dot{m}_f LHV = \dot{m}_g h_3 + 0.03 \dot{m}_f LHV$$

Eq. (5).

Where, subscripts f and g denote fuel and product gas respectively. More details about combustion can be found elsewhere [15]

3.1.3. Gas Turbine (GT):

The gas turbine outlet properties are dependent on gas turbine isentropic efficiency

$$\dot{W}_{GT} = \dot{m}_g (h_3 - h_4) \quad \text{Eq. (6)}$$

The net output power of the Brayton cycle can be expressed as:

$$\dot{W}_{net,GT} = \dot{W}_{GT} - \dot{W}_{AC} \quad \text{Eq. (7)}$$

3.2. Steam Rankine Cycle:

Water steam is generated in the High temperature boiler (HTB) by using hot flue gases leaving the gas turbine. The energy rate balance for the LTB is defined as:

$$\dot{m}_4 (h_4 - h_5) = \dot{m}_9 (h_{10} - h_9) \quad \text{Eq. (8)}$$

The power generation in the cycle is defined as:

$$\dot{W}_{HTT} = \dot{m}_{10} (h_{10} - h_{11}) \quad \text{Eq. (9)}$$

The energy consumed by the pump is defined as:

$$\dot{W}_{HTP} = \dot{m}_8 (h_9 - h_8) \quad \text{Eq. (10)}$$

Accordingly the net power output of the Steam Rankine Cycle is determined as:

$$\dot{W}_{net,HTT} = \dot{W}_{HTT} - \dot{W}_{HTP} \quad \text{Eq. (11)}$$

The heat rejected by the condenser is expressed as:

$$\dot{Q}_{cond} = \dot{m}_{11} (h_{11} - h_8) \quad \text{Eq. (12)}$$

where satisfies the heat pump system's thermal energy.

3.3. Organic Rankine Cycle (ORC):

Cyclohexane vapor is generated in the LTB using hot flue gases leaving the HTB. The energy rate balance.

for the LTB is defined as:

$$\dot{m}_{13} (h_{13} - h_{14}) = \dot{m}_g (h_6 - h_5) \quad \text{Eq. (13)}$$

Power generated by the turbine and energy consumption by the pump are expressed as:

$$\dot{W}_{LTT} = \dot{m}_{14} (h_{14} - h_{15}) \quad \text{Eq. (14)}$$

$$\dot{W}_{LTP} = \dot{m}_{12} (h_{13} - h_{12}) \quad \text{Eq. (15)}$$

The output thermal energy by the ORC condenser is used to produce hot water in 65(°C) for district users that the energy balance defined as below:

3.4. District Hot Water:

$$\dot{m}_8 (h_{12} - h_{15}) = \dot{m}_{25} (h_{25} - h_{26}) \quad \text{Eq. (16)}$$

And the energy consumed by the district hot water pump is expressed as:

$$\dot{W}_{DHW,pump} = \dot{m}_{DHW} (h_{25} - h_{24}) \quad \text{Eq. (17)}$$

Therefore the net power output of ORC turbine is defined as:

$$\dot{W}_{net,LTT} = \dot{W}_{LTT} - \dot{W}_{LTP} - \dot{W}_{comp} - \dot{W}_{DHW,pump} \quad \text{Eq. (18)}$$

3.5. Heat Pump System:

Water evaporates at state 16 and low pressure steam, which enters the compressor. According to Eq. (18), the compressor is driven by work from the ORC turbine. Note that the deaerator pressure is 300 kPa, while the compressor compresses steam to this grade. The demandable energy for compressor shaft working is defined as:

$$\dot{W}_{comp} = \dot{m}_{17} (h_{17} - h_{16}) \quad \text{Eq. (19)}$$

In the deaerator, the compressed high temperature superheated steam mixes with the pumped return water from the district heating network and the final mixed water exits the deaerator to the district heat users. The district heating load is determined as follows:

$$\dot{Q}_{dist} = \dot{m}_{18} (h_{18} - h_{19}) \quad \text{Eq. (20)}$$

The water return pump power consumed is defined as follows:

$$\dot{W}_{D,P} = \dot{m}_{21} (h_{22} - h_{21}) \quad \text{Eq. (21)}$$

3.6. Wind Turbine:

Average power obtained from the wind turbine is expressed as follows: [11]

$$\dot{W}_{wt} = \frac{1}{2} \eta_{wt} \rho_{air} A_{wt} C_p U^3 \quad \text{Eq. (22)}$$

Where η_{wt} is the wind turbine efficiency, ρ_{air} is the air density, A_{wt} is the swept wind turbine area, C_p is the turbine power coefficient, U is the average wind speed.

3.7. Proton Exchange Membrane (PEM) Electrolyzer:

Energy and exergy analyses of a PEM electrolyzer can be performed in conjunction the electrochemical modeling. The total energy demand for PEM electrolysis can be calculated as:

$$\Delta H = \Delta G + T\Delta S \quad \text{Eq. (23)}$$

Where ΔG is the electrical energy demand (change in Gibb's free energy) and $T\Delta S$ is the thermal energy demand (J/molH_2). The values of H, G, and S for H_2 , O_2 , and H_2O can be obtained from the JANAF Table. The total energy need is the theoretical energy required for water electrolysis without any losses. The catalyst used in PEM electrolysis provides an alternative path for the reaction with lower activation energy. The outlet flow rate of H_2 can be determined by:

$$\dot{N}_{\text{H}_2, \text{out}} = \frac{J}{2F} = \dot{N}_{\text{H}_2\text{O}, \text{reacted}} \quad \text{Eq. (24)}$$

Where J is the current density, F is the Faraday constant, and $\dot{N}_{\text{H}_2\text{O}, \text{reacted}}$ is the rate of H_2O reacted in the process (10). The electric energy input rate to the electrolyzer can be expressed as:

$$E_{\text{electric}} = Ex_{\text{electric}} = JV \quad \text{Eq. (25)}$$

Where E_{electric} is the electric energy input and Ex_{electric} the electric exergy input. Also, V is given as:

$$V = V_0 + V_{\text{act}, a} + V_{\text{act}, c} + V_{\text{ohm}} \quad \text{Eq. (26)}$$

Where V_0 is the reversible potential, which is related to the difference in free energy between reactants and products, and V_0 can be obtained by the Nernst equation as follows:

$$V_0 = 1.229 - 8.5 * 10^{-4}(T_{\text{PEM}} - 298.15) \quad \text{Eq. (27)}$$

Also $V_{\text{act}, a}$, $V_{\text{act}, c}$ and V_{ohm} are the activation overpotential of the anode, the activation over potential of the cathode, and the ohmic over potential of the electrolyte, respectively. Ohmic over potential in the proton exchange membrane is caused by the resistance of the membrane to the hydrogen ions transporting through it. The ionic resistance of the membrane depends on the degree of humidification and thickness of the membrane as well as the membrane temperature. The local ionic conductivity $C(x)$ of the proton exchange membrane can be expressed as:

$$C_{\text{PEM}}[\lambda(x)] = [0.5139\lambda(x)0.326] \exp\left[1268\left(\frac{1}{303} - \frac{1}{T}\right)\right] \quad \text{Eq. (28)}$$

Where x is the distance in the membrane measured from the cathode-membrane interface and $\lambda(x)$ is the water content at a location x in the membrane and T is the membrane temperature.

The value of $\lambda(x)$ can be calculated in terms of the water content at the membrane electrode edges:

$$\lambda(x) = \frac{\lambda_a - \lambda_c}{D}x + \lambda_c \quad \text{Eq. (29)}$$

Where D is the membrane thickness, and λ_a and λ_c are the water contents at the anode-membrane and the cathode membrane interfaces, respectively. The overall Ohmic resistance (R_{PEM}) can thus be determined as:

$$R_{\text{PEM}} = \int_0^D \frac{dx}{\sigma_{\text{PEM}}[\lambda(x)]} \quad \text{Eq. (30)}$$

The ohmic over potential can be expressed in terms of Ohm's law:

$$V_{\text{ohm}, \text{PEM}} = JR_{\text{PEM}} \quad \text{Eq. (31)}$$

The activation over potential, V_{act} , caused by a deviation of net current from its equilibrium, and also an electron transfer reaction must be differentiated from the concentration of the oxidized and reduced species Then:

$$V_{\text{act}, i} = \frac{RT}{F} \sinh^{-1} \left(\frac{J}{2J_{0,i}} \right), i = a, c \quad \text{Eq. (32)}$$

Here J_0 is the exchange current density, which is an important parameter in calculating the activation over potential. It characterizes the electrode's capabilities in the electrochemical reaction. A high exchange current density implies a high reactivity of the electrode, which results in a lower over potential. The exchange current density for electrolysis can be expressed as:

$$J_{0,i} = J_i^{\text{ref}} \exp\left(-\frac{E_{\text{act}, i}}{RT}\right), i = a, c \quad \text{Eq. (33)}$$

Where J_i^{ref} is the pre-exponential factor; and $E_{\text{act}, i}$ is the activation energy for anode and cathode, respectively. Further details about PEM electrolysis modeling can be found elsewhere [12, 27].

4. Exergy Balance

When an exergy analysis is performed, the thermodynamic imperfections can be quantified as exergy destructions, which represent losses in energy quality or usefulness (Dincer and Rosen, 2012). The exergy of a substance is often in 4 different forms: physical, chemical, kinetic and potential energy. The last two forms are assumed to be negligible as elevation changes are small and speeds are low. The physical exergy is defined as the maximum theoretical useful work obtained as a system interacts with an equilibrium state. The chemical exergy is associated with the departure of the chemical composition and reaction of a system from its chemical equilibrium.

The chemical exergy is an important part of exergy in combustion processes and chemical reaction. According to the first and the second laws of thermodynamics exergy Balance equation can be written as:

$$\dot{E}x_Q + \sum_i \dot{m}_i ex_i = \sum_e \dot{m}_e ex_e + \dot{E}x_W + \dot{E}x_{dest} \quad \text{Eq. (34)}$$

Where subscripts i and e denote the control volume inlet and outlet flow, respectively and $\dot{E}x_{dest}$ is the exergy destruction rate. Other terms are explained as:

$$\dot{E}x_Q = \left(1 - \frac{T_0}{T_i}\right) \dot{Q}_i \quad \text{Eq. (35)}$$

$$\dot{E}x_W = \dot{W} \quad \text{Eq. (36)}$$

$$Ex = ex_{ph} + ex_{chem} \quad \text{Eq. (37)}$$

$$ex_{ph} = (h - h_0) - T_0(s - s_0) \quad \text{Eq. (38)}$$

where $\dot{E}x_Q$ and $\dot{E}x_W$ are the exergy of heat transfer and work which cross the boundaries of the control volume, T is the absolute temperature and the subscript 0 refers to the reference environment conditions. In Eq. (34-38).

The term $\dot{E}x$ is defined as follows:

$$\dot{E}x = \dot{E}x_{ph} + \dot{E}x_{chem} \quad \text{Eq. (39)}$$

Where

$$\dot{E}x = \dot{m} \cdot ex \quad \text{Eq. (40)}$$

In general, the exergy efficiency is defined as the ratio of the net exergy output to the total exergy input, as follows:

$$\psi = \frac{\dot{E}x_e}{\dot{E}x_i} \quad \text{Eq. (41)}$$

Here, the subscript e denotes product (or net output) and i the overall input exergy to the system or component. This definition applies for most components and the overall system. The quantities described above are given below for each of the system components. Mass and energy rate balances as well as exergy destruction rates resulting from exergy rate balances for each of the system components. Table. 2. lists the exergy destruction rate equation for each component of the system. Energy and exergy efficiencies of the system expressed as:

$$\eta_{system} = \frac{\dot{W}_{net} + \dot{Q}_{dist} + \dot{m}_{25}(h_{26} - h_{25}) + \dot{m}_{H_2} LHV_{H_2}}{\dot{m}_{fuel} LHV_{fuel} + \dot{W}_{wt}} \quad \text{Eq. (42)}$$

$$\psi_{system} = \frac{\dot{W}_{net} + \dot{E}x_{dist} + \dot{E}x_{26} + \dot{E}x_{H_2}}{\dot{E}x_{fuel} + \dot{E}x_{wt}} \quad \text{Eq. (43)}$$

Where:

$$\dot{W}_{net} = \dot{W}_{net,GT} + \dot{W}_{net,HTT} + \dot{W}_{net,LTT}$$

$$\dot{E}x_{dist} = \dot{Q}_{dist} \left(1 - \frac{T_0}{T_{avg}}\right)$$

$$\dot{E}x_{wt} = \frac{1}{2} \rho_{air} A_{wt} U^3$$

Table 2. The expressions used for the system components based on exergy destruction rates.

Component	Exergy destruction rate expression
Air Compressor	$\dot{E}x_{d,AC} = \dot{W}_{AC} - (\dot{E}x_2 - \dot{E}x_1)$
Combustion Chamber	$\dot{E}x_{d,CC} = \dot{m}_a ex_2 + \dot{m}_f ex_f - \dot{Q}_{CC} \left(1 - \frac{T_0}{T_H}\right) - \dot{m}_g ex_g$
Gas Turbine	$\dot{E}x_{d,GT} = (\dot{E}x_3 - \dot{E}x_4) - \dot{W}_{GT}$
Steam Rankine Cycle Pump	$\dot{E}x_{d,HTP} = \dot{W}_{HTP} - (\dot{E}x_9 - \dot{E}x_8)$
Steam Rankine Cycle Boiler	$\dot{E}x_{d,HTB} = \dot{E}x_9 + \dot{E}x_4 - \dot{E}x_{10} - \dot{E}x_5$
Steam Rankine Cycle Turbine	$\dot{E}x_{d,HTT} = (\dot{E}x_{10} - \dot{E}x_{11}) - \dot{W}_{HTT}$
Steam Rankine Cycle Condenser	$\dot{E}x_{d,HTC} = \dot{E}x_{11} + \dot{E}x_{23} - \dot{E}x_8 - \dot{E}x_{16}$
ORC Pump	$\dot{E}x_{d,LTP} = \dot{W}_{LTP} - (\dot{E}x_{13} - \dot{E}x_{12})$
ORC Boiler	$\dot{E}x_{d,LTB} = \dot{E}x_{13} + \dot{E}x_5 - \dot{E}x_{14} - \dot{E}x_6$
ORC Turbine	$\dot{E}x_{d,LTT} = (\dot{E}x_{14} - \dot{E}x_{15}) - \dot{W}_{LTT}$
ORC Condenser	$\dot{E}x_{d,LTC} = \dot{E}x_{15} + \dot{E}x_{25} - \dot{E}x_{12} - \dot{E}x_{26}$
District Hot Water Pump	$\dot{E}x_{d,DWH,pump} = \dot{W}_{DHW,pump} - (\dot{E}x_{25} - \dot{E}x_{24})$
Steam Compressor	$\dot{E}x_{d,comp} = \dot{W}_{comp} - (\dot{E}x_{17} - \dot{E}x_{16})$
Deaerator	$\dot{E}x_{d,dea} = \dot{E}x_{17} - \dot{E}x_{18} - \dot{E}x_{22}$
Expansion Valve	$\dot{E}x_{d,Exp} = \dot{E}x_{20} - \dot{E}x_{23}$
District Return Water Pump	$\dot{E}x_{d,DP} = \dot{W}_{DP} - (\dot{E}x_{22} - \dot{E}x_{21})$
District Users	$\dot{E}x_{d,dist} = (\dot{E}x_{17} - \dot{E}x_{18}) - \dot{Q}_{dist} \left(1 - \frac{T_0}{T_{avg}}\right)$
Wind Turbine	$\dot{E}x_{d,wt} = \dot{W}_{wt} \left(\frac{1}{C_{p,wt}} - 1\right)$
PEM electrolyzer	$\dot{E}x_{d,PEM} = \dot{E}x_{wt} + \dot{E}x_{30} - \dot{E}x_{28} - \dot{E}x_{31}$

5. Environmental Impact

Deducting carbon dioxide emissions, a significant greenhouse gas, as the main factor of environmental impact is increasing the efficiency of energy conversion processes and thereby decreasing fuel consumption. The amount of CO_2 emissions of the overall system is calculated as follows:

$$\epsilon_{system} = \frac{\dot{m}_{CO_2}}{W_{net} + Q_{dist} + \dot{E}_{26} + \dot{E}_{H_2}} \quad \text{Eq. (44).}$$

In order to improve environmental sustainability, it is necessary not only to use sustainable or renewable sources of energy, but also to utilize non-renewable sources like natural gas more

efficiently, while minimizing environmental damage. In this way, the society can reduce its use of limited resources and extend their lifetimes. Here, a sustainability index SI is used to relate exergy with environmental impact

$$SI = \frac{1}{D_P} \quad \text{Eq. (45).}$$

Where D_P is the depletion number, defined as the exergy destruction ratio to input exergy. This relation represents reducing environmental impact of system can be achieved by reducing its exergy destruction.

Table 3. The thermodynamic properties of the system different states.

State	\dot{m} (kg/s)	P (kPa)	T (°C)	h (kJ/kg)	s (kJ/kg K)	ex (kJ/kg)
0		101	25	298.4	6.861	0
1	1.5	101	25	298.4	6.861	0
2	1.5	1212	378.5	662.3	6.948	337.9
3	1.5	1212	1173	1573	7.854	978.3
4	1.5	101	589.3	891.6	7.968	263.3
5	1.5	101	250	527.4	7.433	58.57
6	1.5	101	105.5	379.6	7.102	9.322
7	1.5	101	100	374.1	7.088	8.177
8	0.166	31.18	70	293	0.9549	12.85
9	0.166	2000	70.18	295.4	0.956	14.91
10	0.166	2000	579.3	3644	7.649	1368
11	0.166	31.18	132.9	2748	8.08	343.4
12	0.355	72.5	70	120.5	0.3866	6.149
13	0.355	2000	70.81	123.6	0.388	8.847
14	0.355	2000	240	760.3	1.806	222.6
15	0.355	72.5	160.9	642.9	1.855	90.85
16	0.168	101.3	100	2676	7.354	487.5
17	0.168	270	214.5	2896	7.423	687.4
18	2.121	260	110	461.4	1.418	43.06
19	2.121	150	60	251.3	0.8311	8.022
20	0.168	150	60	251.3	0.8311	8.022
21	1.953	150	60	251.3	0.8311	8.022
22	1.953	270	60.01	251.4	0.8312	8.146
23	0.168	101.3	60.01	251.3	0.8313	7.978
24	0.889	101	15	63.01	0.2242	0.7176
25	0.889	2000	15.1	65.25	0.2254	2.606
26	0.889	2000	65	273.7	0.8924	12.2

Table. 4. Values of the parameters obtained from the system modeling and its energy and exergy analyses.

Parameter		Value
Fuel mass flow rate	\dot{m}_f (kg/s)	0.029
Net output power	$\dot{W}_{net.tot}$ (kW)	1051
District heating load	\dot{Q}_{dist} (kW)	445.8
Hot water mass flow rate	\dot{m}_{DHW} (kg/s)	0.891
Hydrogen production mass flow rate	\dot{m}_{H_2} (kg/h)	2.33
Energy efficiency of the system	η (%)	80.19
Exergy efficiency of system	Ψ (%)	52.63
Total exergy destruction rate	$\dot{E}x_{D.tot}$ (kW)	941
Specific CO ₂ emission	CO ₂ emission (kg/kWh)	0.137
Sustainability index	SI	2.374

6. Results and Discussion

The results of the thermodynamic modeling and analyses are presented here, including assessments of the effects of varying several design parameters on system performance. The thermodynamic properties are presented for states in the system in Table. 3. and the results obtained from the system are tabulated in Table. 4. These outputs are subject to change depending on the parameter that is under consideration.

The effect of variations of several design parameters on the thermodynamic performance of the multi-generation system is assessed. The ambient temperature, air compressor pressure ratio, and average wind speed are some effective parameters in this multi-generation system that we assess them here.

It is shown in Fig. (2). that the effect of ambient temperature on system energy and exergy efficiency levels. For the energy efficiency, increasing ambient temperature is seen to enhance the system energy efficiency. This is mainly due to the corresponding increase in enthalpy of the inlet air to the combustion chamber which enhances net output power, thereby increasing the energy efficiency. Unlike energy efficiency, the exergy efficiency decreases by increasing ambient temperature. This is due to the increase in exergy levels of dead state, which results in lower exergy values for most system states.

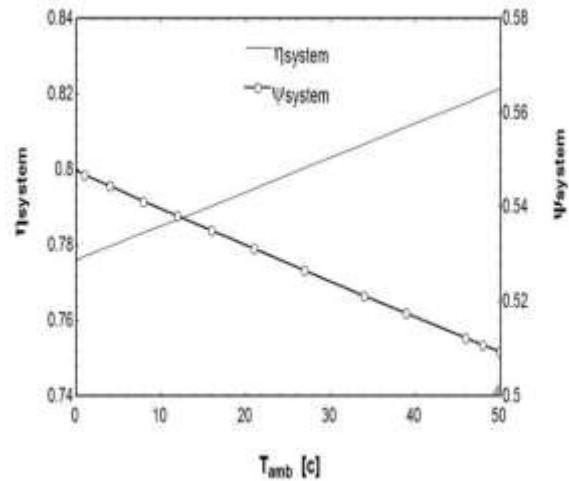


Fig. 2. Effect of ambient temperature on energy and exergy efficiencies.

The variation of sustainability index and exergy destruction of the system by air compressor pressure ratio is shown in Fig. (3). It is seen that the fuel consumption is decreases as pressure ratio increases, mainly due to the increase of the combustion chamber inlet temperature. Thereby total exergy destruction of the system decreases and the sustainability index increases with increasing of the air compressor pressure ratio. Also the variation of fuel consumption influence on carbon dioxide emission. Fig. (4). illustrates how the reduction of the fuel consumption decreases the carbon dioxide emission.

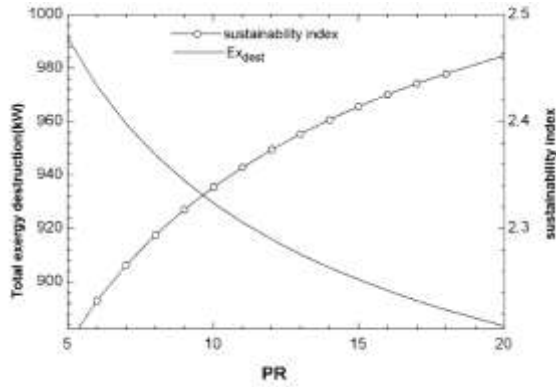


Fig. 3. Variations in the compressor pressure ratio of total exergy destruction rate to sustainability index.

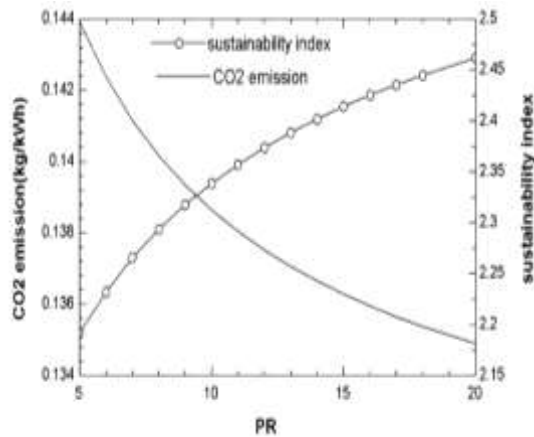


Fig. 4. Variations in the compressor pressure ratio of sustainability index to CO2 emission.

Fig. (5). shows the effect of average wind speed on the total energy and exergy efficiency of the system. It is observed that the multi-generation system exergy efficiency decreases and energy efficiency increases with increasing of average wind speed. This results from increasing wind turbine output power. Similarly the total exergy destruction of the system and sustainability index increase by raising of average wind speed that is shown in Fig. (6).

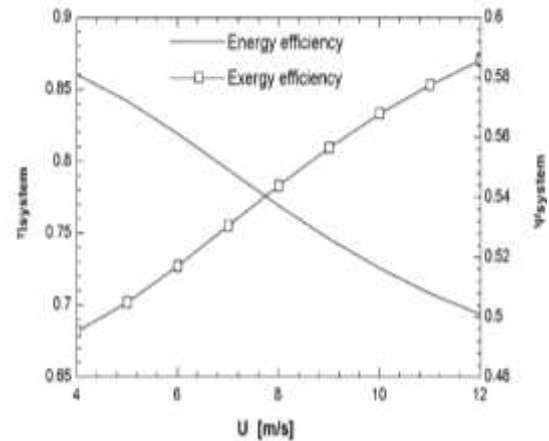


Fig. 5. The effects of average wind speed on the energy and exergy efficiencies.

Table 5. The thermodynamic analysis of the fuel affecting the system.

Fuel	\dot{m}_{fuel} (kg/s)	CO ₂ emission (kg/kWh)	SI	η_{system} (%)	Ψ_{system} (%)	$\dot{E}x_{D,\text{tot}}$ (kW)
Methane(CH_4)	0.029	0.137	2.374	80.19	52.63	941
Ethane(C_2H_6)	0.0306	0.154	2.354	80.18	52.31	965
Propane(C_3H_8)	0.0314	0.162	2.337	80.17	52.04	968
N-Butane(C_4H_{10})	0.0319	0.166	2.331	80.17	51.93	973.1

Table 6. Results of the thermodynamic analysis based on the increasing number of wind turbines.

Number of wind turbine	η_{system} (%)	Ψ_{system} (%)	\dot{m}_{air} (kg/s)	\dot{m}_{fuel} (kg/s)	CO ₂ emission (kg/kWh)	SI	$\dot{E}x_{D,\text{tot}}$ (kW)
1	86.47	49.3	2.201	0.042	0.224	2.122	1153
2	84.49	50.34	1.967	0.0381	0.193	2.195	1083
3	82.41	51.45	1.734	0.0336	0.164	2.278	1012.3
4	80.19	52.63	1.5	0.029	0.137	2.374	941
5	77.82	53.91	1.265	0.0245	0.112	2.486	870.4
6	75.3	55.27	1.032	0.02	0.088	2.619	800.1
7	72.59	56.75	0.796	0.0154	0.066	2.781	728.4
8	69.7	58.34	0.563	0.011	0.045	2.978	658
9	66.6	60	0.329	0.0064	0.026	3.228	586.9
10	63.23	61.94	0.094	0.0018	0.007	3.567	513.5

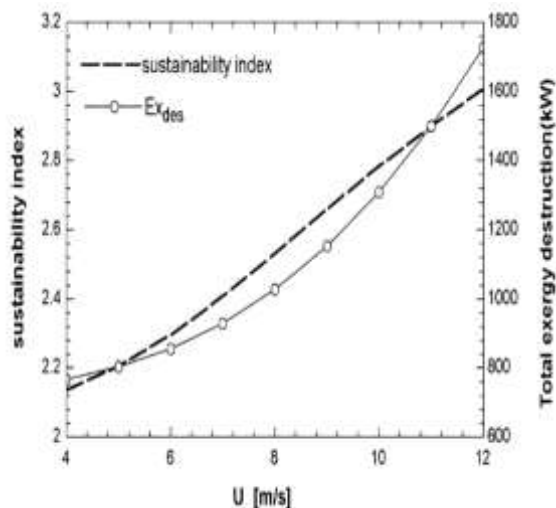


Fig. 6. The effects of average wind speed on the total exergy destruction and sustainability index.

Fuel is one of the significant parameters to studying. There are several fuels to investigate their effect on multi-generation system at constant turbine inlet temperature, where were listed in Table. 5. The effect of fuel change on fuel consumption rate, carbon dioxide emission rate, sustainability index and energy and exergy efficiencies is shown. It is seen that for satisfying specified gas turbine inlet temperature (1173 °C), the methane with 0.029 (kg/s) mass flow rate has the least and n-butane with 0.0319 (kg/s) mass flow rate has the most fuel consumption. Therefore the least environmental impact is related to methane with carbon dioxide emission rate about 0.137 (kg/kWh) and the most impact is related to n-butane with carbon dioxide emission rate about 0.166 (kg/kWh). At last the methane has the most energy and exergy efficiencies and sustainability index for presenting multi-generation energy system. Another subject that we considered in this paper is analyzing of replacing renewable energy system (wind Turbine) with conventional system (gas turbine) for production of specified amount of electricity. Accordingly, we studied the performance of system with increasing number of wind turbine and reducing portion of gas turbine. That is reported in Table 6. It is seen that adding the number of wind turbine (renewable energy) and reducing of conventional system portion for producing specified amount of electricity decrease fossil fuel consumption where affect environmental impact and reduce carbon dioxide emission rate. According to the Table. 6. sustainability index enhanced by increasing the number of wind turbine where it is result of increasing renewable energy portion and exergy destruction rate reduced with decreasing gas turbine portion where it is the cause of reducing combustion chamber role in total system. Thereby the overall exergy efficiency is improved.

7. Conclusion

In a review of exergy losses, the maximum losses are due to combustion chamber. The evaluation of energy losses and its improvement in this chamber is very important for system efficiency. There are two items for improving this problem. One is reducing the difference of inlet and outlet temperature in the combustion chamber by preheating inlet air and the other one is developing the insulation. The gas turbine system is incapacitated. Because in winter, the pressure of the urban gas network will be reduced or omitted. One of the advantages of the studied system is that the produced hydrogen and the reservoir by wind turbine, has been used to fuel cell and prevented power outage. Since the wind turbine required specified range of wind speed for connecting to the network and on the other side due to changes of wind speed, equipment for energy saving and network load stability is required that it cost a lot for preparing and maintenance these, the other advantages of the proposed system is optimum utilization of wind energy by the generation of Hydrogen. The important parameter in this investigation is the ratio of compressor pressure that has significant influence for carbon dioxide diffusion and system stability. So, selection of the compressor type is very important. For fossil fuel, when the ratio of carbon to hydrogen is increased, then air pollution increases and efficiency is decreased.

References

- [1] H. Lund and E. Münster, *Vlo.* 34, (2006), pp. 1152.
- [2] R. Soltani, I. Dincer and M. A. Rosen, *Appl. Therm. Eng.*, Vol. 89, (2015), pp. 90.
- [3] P. Ahmadi, I. Dincer and M. A. Rosen, *Energ. Conv. Manage.*, Vol. 76, (2013), pp. 282.
- [4] T. A. H. Ratlamwala, I. Dincer and M. Gadalla, *Appl. Therm. Eng.*, Vol. 40, (2012), pp. 71.
- [5] P. Ahmadi, I. Dincer and M. A. Rosen, *Energ.*, Vol. 56, (2013), pp. 155.
- [6] P. J. Mago and A. K. Hueffed, *Energ. Build.*, Vol. 42, (2010), pp. 1628.
- [7] S. Ozlu and I. Dincer, *Sol. Energ.*, Vol. 122, (2015), pp. 1279.
- [8] Y. Bicer and I. Dincer, *Energ.*, Vol. 94, (2016), pp. 623.
- [9] R. Soltani, I. Dincer and M. A. Rosen, *Appl. Therm. Eng.*, Vol. 89, (2015), pp. 833.
- [10] M. Ozturk and I. Dincer, *Appl. Therm. Eng.*, Vol. 51, (2013), pp. 1235.
- [11] J. A. Duffie and W. A. Beckman, "Solar Engineering of Thermal Processes", 3rd ed New Jersey, Wiley, (2006).
- [12] M. Ni, M. K. Leung and D. Y. Leung, *Energ. Conv. Manage.*, Vol. 49, (2008), pp. 2748.

- [13] K. J. Chua, S. K. Chou and W. M. Yang, Appl. Energ., Vol. 87, NO. 12, (2010), pp. 3611.
- [14] H. Kurt, Z. Recebli and E. Gredik, Int. J. Energ Res., Vol. 33, NO. 2, (2009), pp. 285.
- [15] S. Mc Allisterl, J. Y. Chen and F. Pello, Springer, New York, (2011).
- [16] P. Ahmadi, I. Dincer and M. A. Rosen, Energ. Convers. Manage., Vol. 64, (2012), pp. 447.
- [17] M. A. Rosen, I. Dincer and M. Kanoglu, Energ. Policy., Vol. 36, NO. 1, (2012), pp. 128.
- [18] R. Soltani, I. Dincer and M. A. Rosen, Energ. Convers. Manage., Vol. 89, (2015), pp. 577.
- [19] P. Ahmadi, I. Dincer and M. A. Rosen, Sol. Energ., Vol. 108, pp. 576-591, (2014).
- [20] M. K. Desmukh and S. S. Desmukh, Renew. Sust. Energ. Rev., Vol. 12, (2008), pp. 235.
- [21] J. C. Bruno, Lopez, J. Villada, E. Letelier, S. Romera and A. Coronas, Appl. Therm. Eng., Vol. 28, (2008), pp 2212.
- [22] M. Esteban and D. Leary, "Developments and Future Prospects of Offshore Wind and Ocean Energy", Appl Energ, Vol 90, pp. 128–136, (2012).
- [23] B. F. Tchanche, G. Lambrinos, A. Frangoudakis and G. Papadakis, Renew. Sust. Energ. Revi., Vol. 15, (2011), pp. 3963.
- [24] R. Salcedo, E. Antipova, D. Boer, L. Jiménez, Guillén and G. Gosálbez, Desalination, Vol. 286, (2012), pp. 358.
- [25] P. Ahmadi and I. Dincer, Appl. Therm. Eng., Vol. 31, (2011), pp. 2529.
- [26] A. B. Little and S. Garimella, Energy, Vol. 36, (2011), pp. 4492.
- [27] P. Ahmadi and I. Dincer and M. A. Rosen, Int. J. Hydrog. Energ., Vol. 38, (2013), pp. 1795.
- [28] D. Lewis, "Cold Climate Air-Source Heat Pump", US, Patent , 7266959 B2. <http://www.google.com/patents/US7266959>; 2007 [15 July 2014].
- [29] I. Dincer and M. A. Rosen, Elsevier Sci., (2012).

Nomenclature			
A	area, m^2	$Chem$	chemical
C_p	wind turbine power coefficient	$comp$	compressor
D_p	depletion number	$dest$	destruction
\dot{E}	energy rate (kW)	DHW	district hot water
\dot{E}_x	exergy rate (kW)	$dist$	district
F	Faraday constant, C/mol	DP	deaerator pump
G	Gibb's free energy, kJ	e	outlet condition
H	specific enthalpy, kJ/kg	f	Fuel
J	current density, A/m^2	G	gas turbine outlet gas
LHV	lower heating value, kJ/kg	GT	gas turbine
\dot{m}	Mass flow rate, kg/s	HTP	high temperature pump
\dot{N}	molar mass flow rate, mol/s	HTT	high temperature turbine
\dot{Q}	heat transfer rate, kW	i	inlet condition
R_{PEM}	proton exchange membrane resistance, Ω	LTP	low temperature pump
S	specific entropy, kJ/kg K	LTT	low temperature turbine
SI	sustainable index	ph	physical
T	temperature, K	wt	wind turbine
U	velocity, m/s		
V	voltage potential, V	$Greek\ letters$	
\dot{W}	work rate, kW	ε	normalized CO_2 emissions, kg/MWh
		η	energy efficiency
<i>Subscripts</i>		λ	water content at location x in the membrane, Ω^{-1}
a	air	ρ	density
AC	air compressor	ψ	exergy efficiency